


# Adaptive Imaging Versus Periodic Surveillance for Intrafraction Motion Management During Prostate Cancer Radiotherapy

Technology in Cancer Research & Treatment  
 Volume 18: 1-8  
 © The Author(s) 2019  
 Article reuse guidelines:  
[sagepub.com/journals-permissions](http://sagepub.com/journals-permissions)  
 DOI: 10.1177/1533033819844489  
[journals.sagepub.com/home/tct](http://journals.sagepub.com/home/tct)  


Xiangyu Ma, MS<sup>1,2,3</sup> , Huagang Yan, PhD<sup>1,2</sup>, Ravinder Nath, PhD<sup>2</sup>, Zhe Chen, PhD<sup>2</sup>, Haiyun Li, PhD<sup>1,3</sup>, and Wu Liu, PhD<sup>2</sup>

## Abstract

**Objective:** To evaluate the benefits of adaptive imaging with automatic correction compared to periodic surveillance strategies with either manual or automatic correction. **Methods:** Using Calypso trajectories from 54 patients with prostate cancer at 2 institutions, we simulated 5-field intensity-modulated radiation therapy and dual-arc volumetric-modulated arc therapy with periodic imaging at various frequencies and with continuous adaptive imaging, respectively. With manual/automatic correction, we assumed there was a 30/1 second delay after imaging to determine and apply couch shift. For adaptive imaging, real-time “dose-free” cine-MV images during beam delivery are used in conjunction with online-updated motion pattern information to estimate 3D displacement. Simultaneous MV-kV imaging is only used to confirm the estimated overthreshold motion and calculate couch shift, hence very low additional patient dose from kV imaging. **Results:** Without intrafraction intervention, the prostates could on average have moved out of a 3-mm margin for ~20% of the beam-on time after setup imaging in current clinical situation. If the time interval from the setup imaging to beam-on can be reduced to only 30 seconds, the mean over-3 mm percentage can be reduced to ~7%. For intensity-modulated radiation therapy simulation, with manual correction, 110 and 70 seconds imaging periods both reduced the mean over-3 mm time to ~4%. Automatic correction could give another 1% to 2% improvement. However, with either manual or automatic correction, the maximum patient-specific over-3 mm time was still relatively high (from 6.4% to 12.6%) and those patients are actually clinically most important. In contrast, adaptive imaging with automatic intervention significantly reduced the mean percentage to 0.6% and the maximum to 2.7% and averagely only ~1 kV image and ~1 couch shift were needed per fraction. The results of volumetric-modulated arc therapy simulation show a similar trend to that of intensity-modulated radiation therapy. **Conclusions:** Adaptive continuous monitoring with automatic motion compensation is more beneficial than periodic imaging surveillance at similar or even less imaging dose.

## Keywords

intrafraction motion management, portal imaging, on-board kV imaging, image-guided radiation therapy, imaging dose

## Abbreviations

AMI, adaptive monitoring and intervention; AP, anterior–posterior; CMI, continuous monitoring and intervention; IMRT, intensity-modulated radiation therapy; NI, no intervention; PMI, periodic monitoring and intervention; SI, superior–inferior; VMAT, volumetric-modulated arc therapy; PTV, planning target volume.

Received: July 08, 2018; Revised: February 10, 2019; Accepted: March 26, 2019.

## Introduction

The hypofractionated regimen has drawn increasing attention for prostate cancer radiotherapy due to the much lower  $\alpha/\beta$  ratio for prostate cancer than that for other cancers.<sup>1</sup> If not implemented accurately, however, a dramatically higher dose in single fraction than conventional fractionated treatment could increase the risk of delivering a high radiation dose to surrounding organs. It could lead to complications such as

<sup>1</sup> School of Biomedical Engineering, Capital Medical University, Beijing, China

<sup>2</sup> Department of Therapeutic Radiology, Yale University School of Medicine and Yale-New Haven Hospital, New Haven, CT, USA

<sup>3</sup> Beijing Key Laboratory of Fundamental Research on Biomechanics in Clinical Application, Capital Medical University, Beijing, China

## Corresponding Authors:

Wu Liu, PhD, Department of Therapeutic Radiology, Yale University School of Medicine and Yale-New Haven Hospital, New Haven, CT, USA.  
 Email: [wu.liu@yale.edu](mailto:wu.liu@yale.edu)

Haiyun Li, PhD, School of Biomedical Engineering, Capital Medical University, Beijing 100069, China.  
 Email: [haiyunli@ccmu.edu.cn](mailto:haiyunli@ccmu.edu.cn)



acute radiation proctitis,<sup>2,3</sup> which is a negative determinant of the patient's quality of life after treatment.<sup>4</sup> Tight planning target volume (PTV) margin is required for the hypofractionated regimen to escalate target dose and reduce the dose to nearby tissues. Image-guided patient setup can significantly reduce interfraction uncertainty. However, the movement of organs surrounding the prostate (e.g., bladder and rectum fillings) can impact both interfraction and intrafraction prostate positioning. Schild *et al*<sup>5</sup> found that the distension of rectum (bladder) could shift the prostate posterior margin anteriorly (posteriorly) for more than 1 (2) mm for 50% patients and even more than 5 mm for 17% (9%) patients. Boda-Hegemann *et al*<sup>6</sup> found the median of overall prostate intrafraction displacement to be about 3 mm. With a 3 to 5 mm PTV margin, the dosimetric consequences of both interfraction and intrafraction motion are critical.<sup>1,4</sup> If intrafraction motion is not handled well, it may lead to target underdosing and/or normal tissue complications.<sup>7,8</sup>

To deal with intrafraction motion, antifatulent diets had been proposed in order to reduce/suppress the intrafraction motion amplitudes. However, studies showed it was not effective and thus it's not recommended for the purpose of intrafraction motion reduction.<sup>9,10</sup> Real-time motion management techniques are often implemented to compensate the intrafraction prostate motion. For example, with Calypso (Varian Medical Systems, Palo Alto, California) electromagnetic tracking system, one can acquire real-time 3D target positions by localizing the centroids of the implanted electromagnetic transponders and do interventions depending on the motion amplitude. This continuous monitoring and intervention (CMI) method has been proved to be clinically superior to conventional image-guided radiotherapy without intrafraction motion management in terms of PTV coverage.<sup>1</sup> However, Calypso system is expensive and not widely available, and Calypso beacons produce severe magnetic resonance artifacts on follow-up magnetic resonance imaging scans. Alternatively, on-board kV and MV portal imaging systems are standard for modern linacs. Continuous fluorescent kV imaging can be used to monitor the prostate motion of patients with implanted gold markers. Keall *et al*<sup>11</sup> reported clinical treatment using continuous kV intrafraction monitoring and achieved submillimeter treatment accuracy and precision. However, continuous kV imaging imposes excessive imaging dose to the patient.

As a trade-off between no intervention (NI) and CMI, one may implement periodic monitoring and intervention (PMI) which involves imaging between/during beam deliveries. Nonetheless, PMI is "blind" to the motion during the imaging intervals. Apart from this intrinsic limitation, the choice of the imaging frequency becomes another difficult problem and often be treated empirically. Curtis *et al*<sup>12</sup> investigated PTV margin as a function of imaging and correction frequency and provided reference frequencies for different PTV margins. They, however, assumed in their calculation that the prostate displacement was corrected instantaneously at the time of imaging. In current clinical situation without automatic motion

correction, it takes up to 1 minute after imaging to manually decide and apply the couch shift.<sup>1</sup> With such a delay, the detected displacements may have changed considerably when the repositioning is actually performed, thus the management effectiveness is possibly undermined.<sup>13,14</sup>

To overcome the limitation of the aforementioned methods, we previously developed a failure detection method.<sup>15</sup> It is an adaptive monitoring and intervention (AMI) strategy that uses continuous dose-free cine MV portal imaging during the treatment beam delivery and as-needed on-board kV imaging. At present, a systematic comparison among NI, PMI, and AMI strategies is absent in the literature. In this study, by treatment simulations and quantitative comparisons, we demonstrate the benefit of AMI strategy combined with automatic motion compensation during fixed-gantry intensity-modulated radiation therapy (IMRT) and volumetric-modulated arc therapy (VMAT).

## Materials and Methods

### Clinical Data

The motion monitoring methods were evaluated by computer simulation using retrospective real-time 3D prostate position data recorded with implanted electromagnetic transponders (Calypso) from 37 patients treated at Yale (data set 1) and 17 patients treated at MD Anderson<sup>16</sup> (data set 2). This study uses deidentified retrospective data therefore institutional review and written consent are exempted. There are 3011 prostate motion tracks in the 2 data sets. The mean/min/max track length is 276/2/1018 seconds for data set 1 and 338/1/1114 seconds for data set 2. Short and incomplete tracks were removed based on the lengths needed for the simulations. Therefore, 1881 tracks (length >270 seconds) were included in the IMRT simulations and 1669 tracks (length >284 seconds) were included in the VMAT simulations. The prostate motion distributions of the 2 data sets are shown in Figure 1. Since the motion amplitude distributions of the 2 data sets are similar, the 2 data sets were merged for the subsequent simulations.

Five-field fixed-gantry IMRT and dual-arc VMAT deliveries were simulated by applying NI, PMI, and AMI strategies, respectively. Table 1 lists the simulation parameters. The percentage of time that the target moved from the ideal planned position by more than a 3-mm threshold was calculated for each motion management strategy, as well as the root mean square displacement. The number of kV imaging is also calculated to evaluate the additional patient imaging dose.

### No Intervention

For NI strategy, setup imaging and patient positioning were performed only at the beginning of each fraction and intrafraction motion was not monitored. We simulated 30 seconds, 1 minute, 2 minute, and 3 minute delays for manual setup. The

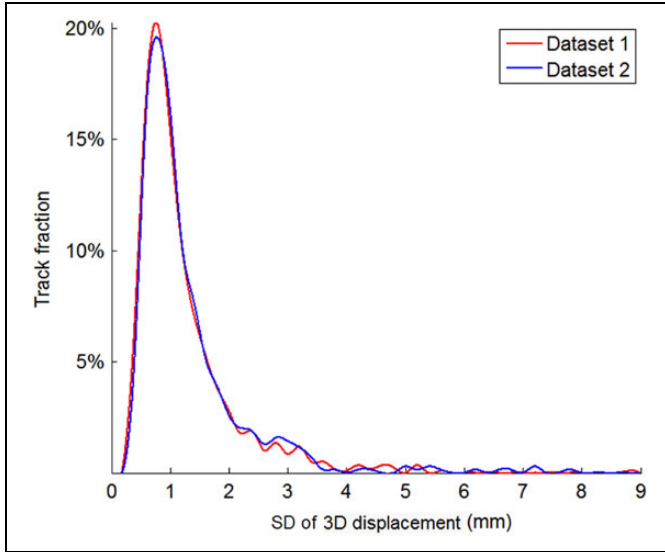


**Figure 1.** Proportion of tracks with different motion amplitudes in the 2 data sets. The amplitude is measured by the standard deviation of the 3D displacement during the first 330 seconds of each track, which is the maximal length used in our simulations.

**Table 1.** Protocols of IMRT and VMAT Simulations.

Five-field fixed-gantry IMRT	Gantry angles (IEC scale) of the fields ( $^{\circ}$ )	Beam-on time for each field (s)	Interval between fields (s)
	255/315/0/45/105	20	20
Dual-arc VMAT	Gantry speed ( $^{\circ}/s$ )	Beam-on time for each arc (s)	Interval between arcs (s)
	5	72	20

Abbreviations: IEC, International Electrotechnical Commission; IMRT, intensity-modulated radiation therapy; VMAT, volumetric-modulated arc therapy.

delay accounts for the time needed after imaging to determine the target displacement and then apply the couch shift accordingly.

### Periodic Monitoring and Intervention

For 5-field fixed-gantry IMRT, we evaluated 2 PMI strategies: imaging before the first, third, and fifth field (low imaging frequency) or imaging before each field (high imaging frequency). For dual-arc VMAT, we also evaluated 2 strategies: imaging before each arc (low imaging frequency) or imaging before and at the middle of each arc (high imaging frequency). One second and 30 seconds intervention delays were assumed for automatic and manual intervention, respectively. A 2.5 mm correction threshold was used to determine whether a repositioning should be performed for a 3D displacement detected by simultaneous MV-kV stereoscopic imaging.<sup>17</sup>

### Adaptive Monitoring and Intervention

The AMI strategy used in this study is an improved version of the “failure detection” strategy proposed in our previous work.<sup>15</sup> It starts with a setup MV-kV stereoscopic imaging pair and couch alignment based on the imaged target position. Cine-MV images are collected continuously during the radiation treatment and kV images are acquired occasionally as-needed based on the MV-estimated target displacement. Target position was estimated in real-time through one of the 2 forms: (1) 2D-to-3D estimation and (2) triangulation of current MV image with a reference image. For the 2D-to-3D estimation, cine-MV images, combined with prior knowledge of the prostate motion, were utilized to estimate the real-time target position. The prior knowledge is based on the population-based assumption that the displacements along anterior–posterior (AP) and superior–inferior (SI) directions, denoted  $\delta_{AP}$  and  $\delta_{SI}$ , respectively, are strongly correlated, hence a relatively stable displacement ratio  $\eta = \frac{\delta_{AP}}{\delta_{SI}}$ . Besides, the amplitude of left-right motion is assumed to be much smaller than that of the other 2 directions. This assumption has been proved by many studies<sup>12,18,19</sup> and is consistent with the pelvis and prostate anatomy,<sup>15</sup> therefore can be conveniently adopted to assist 3D position estimation based on the 2D information for real-time applications. As the displacement of SI direction is always parallel to the imager for coplanar delivery, it can be accurately measured by localizing the 2D target on MV images. Then with the ratio of AP/SI, the displacement of AP direction ( $\delta_{AP}$ ) can be estimated and the displacement perpendicular to the MV imager ( $\delta_{\perp}$ ) can be further estimated as:

$$\delta_{\perp} = \eta \delta_{SI} \cos \alpha$$

where  $\alpha$  is the gantry angle. The 2 coordinates of the target projection in the MV imager plane and the estimated target coordinate perpendicular to the imager can be regarded as the target 3D coordinates in the MV imager coordinate system, and the machine coordinates of the target can be obtained by rigid coordinate transformation from the MV imager to the machine. In addition to the above 2D-to-3D estimation, we also estimated the 3D displacement from the isocenter using the triangulation between the current MV image and a reference position which is orthogonally projected from the 3D target position that has been measured using the latest MV-kV triangulation. The final estimated displacement was the larger one between the 2D-to-3D estimation and the triangulation estimation.

The displacement estimation is intended to be rough and fast. If the estimated displacement exceeds a preset tolerance (2.5mm in this study), kV imaging is triggered to measure the actual 3D displacement by simultaneous MV-kV imaging. Meanwhile, the AP/SI ratio  $\eta$  and the reference position are updated. If the actual 3D displacement is confirmed to be larger than the predetermined correction threshold (2.5 mm in this study), an automatic couch correction is conducted. In addition, due to the 2D-to-3D estimation error, sometimes kV imaging might be repeatedly triggered within a short time, but it turns

out to be a series of “false alarms” (not reaching the correction threshold). To overcome this problem, the correction threshold is designed to follow a “decrease until action” rule, that is, the correction threshold decreases step by step when kV imaging is triggered until a correction is performed and then the threshold returns to its initial value. Because of the “real-time” characteristic of the AMI strategy, long correction delay is not suitable for it, so we simulated the AMI strategy only with automatic couch correction.

## Results

### Representative Single-Track Case

To provide an intuitive comparison of the performance among different motion management strategies, we show a representative single-track IMRT simulation in Figure 2. Assuming a 30 seconds delay from the setup imaging to the beginning of the beam delivery and no intrafraction intervention (Figure 2A), the target gradually moved away from the isocenter during the treatment, resulting in 71.5% overthreshold (3 mm) time. The value is 63.8%/13.7% using lower/higher imaging frequency PMI strategy with manual correction (Figure 2B and C). If the AMI strategy is used, the percentage of overthreshold time can be reduced to only 1.6%, achieved by adaptively using 6 kV images and 3 automatic corrections (Figure 2D).

### Patient-Specific Results

The percentage of overthreshold time was calculated for each track and then averaged for each patient. In general, the results show similar trend for IMRT and VMAT. Without intrafraction intervention, the percentage of overthreshold time increases with setup delay as shown in Table 2.

As shown in Tables 3 and 4, compared with the NI strategy, the use of low-frequency PMI strategy approximately reduces the percentage of overthreshold time by half. At the cost of more imaging dose, high-frequency PMI strategy gives further but moderate improvement to the performance. Adaptive monitoring and intervention strategy provides the best performance with the mean percentage of overthreshold time <1% and the maximum <3% for both IMRT and VMAT scenarios.

In VMAT simulation, on average, the AMI strategy takes about only 1 kV imaging per fraction to achieve mean and maximum over-3 mm time of 0.4% and 1.8% (the last row in Table 4), respectively. In contrast, with 1 kV imaging at the middle of the treatment, that is, with similar imaging dose, the low frequency PMI strategy only achieved the mean over-3 mm time of 4.7%/3.0% and the maximum of 14.4%/11.5% with manual/auto correction (the first 2 rows in Table 4), respectively.

## Discussion

This study simulated fixed-gantry IMRT and VMAT treatment of prostate cancer with different imaging-based motion management strategies.

No intervention strategy with manual setup correction is the most commonly used in current clinical practice. Our results show that its performance has a significant negative correlation with the setup delay. For some patients, the target stays outside the 3 mm margin for the majority of the time, which is clinically unacceptable when tight margin (3 mm or less) is used. This is not only due to the error between the displacement detected by setup imaging and the actually corrected displacement by couch shift but also due to the involuntary physiological motion that increases as the treatment time increases. The setup delay of 30 seconds (from the setup imaging to the beginning of the beam delivery) used in our simulation for manual motion compensation is likely to be the fastest possible in clinical practice, therefore our simulation represents the best accuracy achievable without intrafraction motion management. A previous prostate motion management study reported the median of setup delay was 6 minutes and 40 seconds in their clinical settings.<sup>1</sup> They suggested that, if intrafraction motion is not managed, the posterior PTV margin needs to be increased by 2 mm for every additional 5 minute whole treatment duration to ensure 95% of the dose is delivered to the target. Our study verified their finding and suggested that NI strategy is not clinically appropriate if a tight margin is used.

For PMI strategy, the choice of the period of imaging is crucial. Curtis *et al*<sup>12</sup> suggested that imaging every 240 seconds for 3 mm PTV margin can cover the target for 95% of the treatment time. They assumed that the prostate displacement was corrected instantaneously at the imaging time. Practically, to achieve adequate coverage, the imaging interval of 240 seconds may not be adequate if correction delay is taken into account. Using higher imaging and intervention frequency can theoretically improve the motion management performance because it is more likely to capture and correct large displacement in time. However, with manual intervention even at a short 30 seconds delay, the benefit of more frequent imaging may be heavily compromised. As shown in Tables 3 and 4, the PMI2 + manual strategy did not significantly outperform the PMI1 + manual. Besides, more manual interventions prolong the treatment time. In practice, manual intrafraction intervention delay can be 104 ( $\pm$  50) seconds with Calypso real-time tracking system<sup>18</sup> and much longer ( $\sim$ 400 seconds) with image-based correction.<sup>1</sup> With such a delay, it is practically not possible to achieve the desired target coverage by manual periodic surveillance imaging. Therefore, shortening the intrafraction intervention delay is essential for applying high imaging frequency PMI strategies.

However, even with the automatic couch correction (1 second correction delay) and 80 seconds imaging interval, which is much shorter than the 240 seconds suggested by Curtis *et al*,<sup>12</sup> the maximal patient-specific percentage of over-3 mm time with PMI is 10.9% (the second row in Table 3) for IMRT and 11.5% for VMAT (the second row in Table 4). That is, the PMI strategy is never able to effectively deal with the large intrafraction motion in some patients, and the patients with high percentages of overthreshold time are exactly the patients who need effective motion management. The reason,

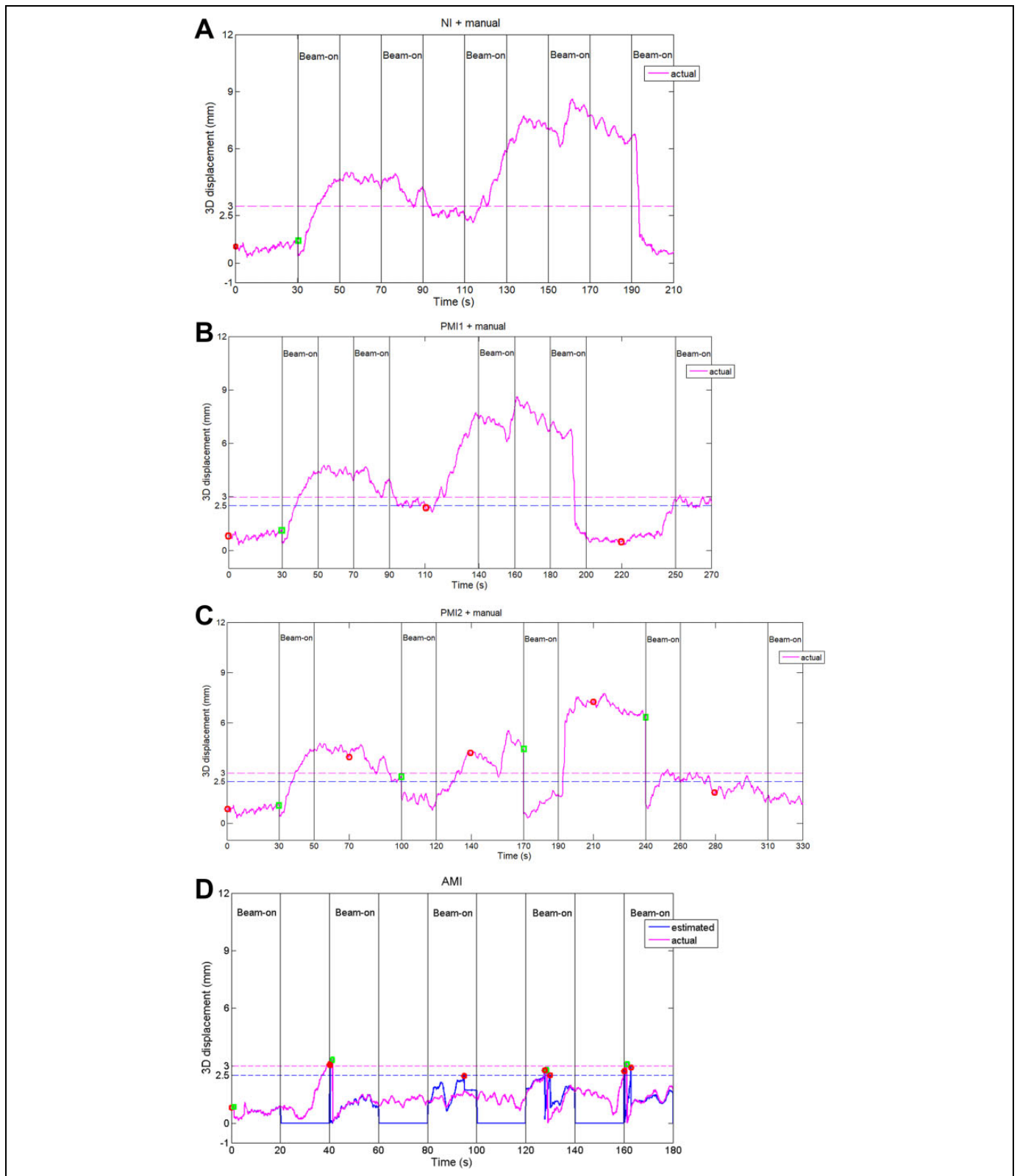


**Figure 2.** An example of motion management for 5-field IMRT delivery using (A) NI with manual setup, (B) PMI1 (low imaging frequency—imaging before the first, third, and fifth field) with manual correction, (C) PMI2 (high imaging frequency—imaging before each field) with manual correction, and (D) AMI strategy. Magenta curves represent the actual 3D displacement of the target and the blue curve in (D) represents the 3D displacement estimated using the cine MV images. The red circle symbols show the time at which kV imaging occurred according to the different estimation algorithms, and the green square symbols denote the couch repositioning events determined by simultaneous MV-kV triangulation. AMI indicates adaptive monitoring and intervention; IMRT, intensity-modulated radiation therapy; NI, no intervention; PMI, periodic monitoring and intervention.

**Table 2.** Patient-Specific Percentage of Over-3 mm Time Using NI Strategy With Different Setup Delays.

Setup Delay (sec)		30	60	120	180
Percentage of overthreshold time, mean (standard deviation), max, (%)	IMRT	6.9 (7.1), 33.1	8.2 (8.5), 44.0	9.3 (10.4), 66.3	19.0 (22.3), 70.0
	VMAT	7.1 (7.2), 31.1	8.5 (8.7), 42.9	11.3 (12.0), 66.8	17.0 (19.3), 77.3

Abbreviations: IMRT, intensity-modulated radiation therapy; NI, no intervention; VMAT, volumetric-modulated arc therapy.

**Table 3.** Patient-Specific Results of AMI and PMI Motion Management Strategies With Manual or Automatic Correction for 5-Field IMRT Simulation.<sup>a</sup>

IMRT	Percentage of Over-3 mm Time (%)		Mean RMS Error (mm)	Number <sup>b</sup> of kV-on per Track		Number <sup>b</sup> of Intervention per Track	
	Mean	Max		Mean	Max	Mean	Max
PMI1 <sup>c</sup> + manual	3.9 ± 4.1	12.6	1.2 ± 0.2	2	2	0.08 ± 0.13	0.35
PMI1 + auto	2.7 ± 3.9	10.9	1.0 ± 0.2	2	2	0.06 ± 0.08	0.23
PMI2 <sup>d</sup> + manual	3.8 ± 2.4	8.9	1.5 ± 0.3	4	4	0.09 ± 0.16	0.43
PMI2 + auto	1.8 ± 2.2	6.4	1.2 ± 0.4	4	4	0.08 ± 0.15	0.39
AMI + auto	0.6 ± 1.0	2.7	0.3 ± 0.1	0.9 ± 0.9	2.7	0.7 ± 0.8	2.3

Abbreviations: AMI, adaptive monitoring and intervention; IMRT, intensity-modulated radiation therapy; PMI, periodic monitoring and intervention; RMS, root mean square.

<sup>a</sup>The delays for manual and auto corrections are assumed to be 30 and 1 second, respectively.

<sup>b</sup>Setup imaging and correction were not counted in the last 2 columns.

<sup>c</sup>PMI1: imaging before the first, third, and fifth field, corresponding to 1 imaging per 110 (80) seconds with manual (auto) correction.

<sup>d</sup>PMI2: imaging before each field, corresponding to 1 imaging per 70 (40) seconds with manual (auto) correction.

**Table 4.** Patient-Specific Results of AMI and PMI Motion Management Strategies With Manual or Automatic Correction for Dual-Arc VMAT Simulation.<sup>a</sup>

VMAT	Percentage of Over-3 mm Time (%)		Mean RMS error (mm)	Number <sup>b</sup> of kV-on per Track		Number <sup>b</sup> of Intervention per Track	
	Mean	Max		Mean	Max	Mean	Max
PMI1 <sup>c</sup> + manual	4.7 ± 4.6	14.4	1.2 ± 0.2	1	1	0.04 ± 0.05	0.15
PMI1 + auto	3.0 ± 4.0	11.5	1.0 ± 0.2	1	1	0.04 ± 0.06	0.16
PMI2 <sup>d</sup> + manual	3.7 ± 5.3	14.8	1.4 ± 0.2	3	3	0.07 ± 0.12	0.32
PMI2 + auto	1.7 ± 2.2	6.3	1.0 ± 0.3	3	3	0.07 ± 0.07	0.23
AMI + auto	0.4 ± 0.7	1.8	0.3 ± 0.1	1.2 ± 1.0	3.4	0.8 ± 0.8	2.5

Abbreviations: AMI, adaptive monitoring and intervention; VMAT, volumetric-modulated arc therapy; PMI, periodic monitoring and intervention; RMS, root mean square.

<sup>a</sup>The setup delays for manual and auto corrections are assumed to be 30 and 1 seconds, respectively.

<sup>b</sup>Setup imaging and correction were not counted in the last 2 columns.

<sup>c</sup>PMI1: imaging before each arc, corresponding to 1 imaging per 122 (92) seconds with manual (auto) correction.

<sup>d</sup>PMI2: imaging before and at the middle of each arc, corresponding to 1 imaging per 86 (56) seconds with manual (auto) correction.

on one hand, is that a generic preset imaging interval that could achieve desirable target coverage for all patients might not exist. On the other hand, this is due to the inherent limitation of PMI strategies, that is, the motion management system is blind during the beam delivery. In addition, the last 2 columns of PMI strategies in Tables 3 and 4 indicate that only a small fraction (less than 5%) of intrafraction kV imaging detected true overthreshold displacement. Thus the imaging dose was not efficiently utilized.

Compared with the CMI and PMI methods, the novelty of the proposed AMI strategy is that it treats the monitoring issue in an adaptive manner, making the motion compensation more

efficient and reducing unnecessary imaging dose. For the IMRT protocol, compared with higher imaging frequency manual PMI strategy, the AMI strategy reduced the maximum percentage of overthreshold time from 8.9% to 2.7% with only one-third of the imaging dose of the former. And for the VMAT protocol, it was from 14.8% to 1.8% with only a quarter of the imaging dose. It can be inferred from the last row of Tables 3 and 4 that averagely about 78% (0.7/0.9) kV images for IMRT simulation and 67% (0.8/1.2) kV images for VMAT simulation were able to capture true large displacement and trigger auto-correction. This demonstrates that the imaging dose utilization efficiency is high with AMI strategy.



Potential problems for cine-MV imaging-based intrafraction monitoring include the multi-leaf collimator (MLC) blockage and target detection (marker-based<sup>20</sup> or soft tissue feature-based<sup>21</sup>) in low-contrast MV images. To deal with the MLC blockage, Ma *et al*<sup>22</sup> proposed a fiducial blockage avoidance strategy in treatment planning phase, and Zhao *et al*<sup>23</sup> developed a leaf-setting algorithm that generates leaf trajectories for dynamic MLCs to achieve maximal marker visibility. For low-contrast marker detection in cine MV images, we previously developed a fast real-time marker tracking algorithm based on discrimination analysis and mean-shift feature space analysis and achieved a tracking error of approximately 0.5 mm.<sup>24</sup> We also developed a markerless tissue-feature detection algorithm for soft tissue positioning based on the identification and auto-association of tissue features contained in the projection images by using scale-invariant feature transform descriptor and showed that the clinical results were promising with the mean error less than 0.5 mm.<sup>20</sup> In addition, recent techniques such as MV short-arc digital tomosynthesis can be used to improve the quality of MV images.<sup>21</sup> Besides, in order to fully integrate AMI into clinical practice, interfaces from the linac manufacturers are also needed so that real-time image processing for target/marker detection, real-time control of the MV and kV image acquisition, and real-time control of couch motion can be implemented on the treatment machine.

In our simulations, we assume the motion pattern is not affected by interventions (e.g., couch shifts). However, interventions do have the possibility to cause prostate motion because they are stimuli to the patients. Although AMI attempts to compensate all overthreshold displacements regardless of their sources, too many interventions may disturb the patients and cause additional motion. Making the couch shift more smoothly instead of an abrupt motion and educating the patients to relax while refraining from voluntary motion may be helpful to eliminate/reduce patients' reactions to the interventions. A prospective study is required to further evaluate the actual performance of the adaptive protocol in clinical settings and analyze patients' reactions to the automatic motion compensation.

Intrafraction motion management with the proposed AMI strategy is more important for stereotactic radiotherapy than conventional fractionated regimens due to higher delivery accuracy requirement. Adaptive imaging is also expected to be useful for conventional fractionated radiotherapy, although smearing the dose in many fractions may alleviate the requirement of delivery accuracy. For conventional fractionated radiotherapy, larger correction thresholds may be used to balance the motion management complexity versus the targeting accuracy. Detailed dosimetric studies are needed to decide the detection and action thresholds appropriate for different applications, similar to the approach suggested in the study by Zhang *et al*.<sup>25</sup>

## Conclusions

Real-time motion monitoring is essential for prostate motion management and it can be implemented by our adaptive

imaging method with low imaging dose. Automatic intervention outperforms manual intervention because it minimizes the time from the detection of an overthreshold event to the execution of motion correction (therefore minimizes the possible additional displacement) and shortens the overall treatment duration. Adaptive imaging combined with automatic motion compensation is more beneficial in terms of target coverage than manual periodic imaging surveillance with similar or even less imaging dose. This finding can be used to guide clinical motion management practice and development.

## Acknowledgment

The authors thank Varian Medical Systems (Palo Alto, California) for providing research software to extract raw Calypso patient data acquired at Yale and Drs P. Kupelian and K. Langen for providing their Calypso data acquired at MD Anderson.

## Declaration of Conflicting Interests

The author(s) declared no potential conflicts of interest with respect to the research, authorship, and/or publication of this article.

## Funding

The author(s) received no financial support for the research, authorship, and/or publication of this article.

## ORCID iD

Xiangyu Ma, MS  <https://orcid.org/0000-0002-9322-1640>

## References

1. Lovelock DM, Messineo AP, Cox BW, Kollmeier MA, Zelefsky MJ. Continuous monitoring and intrafraction target position correction during treatment improves target coverage for patients undergoing SBRT prostate therapy. *Int J Radiat Oncol Biol Phys*. 2015;91(3):588-594.
2. Arcangeli S, Strigari L, Soete G, et al. Clinical and dosimetric predictors of acute toxicity after a 4-week hypofractionated external beam radiotherapy regimen for prostate cancer: results from a multicentric prospective trial. *Int J Radiat Oncol Biol Phys*. 2009; 73(1):39-45.
3. Matzinger O, Duclos F, van den Bergh A, et al. Acute toxicity of curative radiotherapy for intermediate- and high-risk localised prostate cancer in the EORTC trial 22991. *Eur J Cancer*. 2009; 45(16):2825-2834.
4. Paydar I, Cyr RA, Yung TM, et al. Proctitis 1 week after stereotactic body radiation therapy for prostate cancer: implications for clinical trial design. *Front Oncol*. 2016;6:167.
5. Schild SE, Casale HE, Bellefontaine LP. Movements of the prostate due to rectal and bladder distension: implications for radiotherapy. *Med Dosim*. 1993;18(1):3.
6. Boda-Heggemann J, Kohler FM, Wertz H, et al. Intrafraction motion of the prostate during an IMRT session: a fiducial-based 3D measurement with cone-beam CT. *Radiat Oncol*. 2008;3:37.
7. Budaus L, Bolla M, Bossi A, et al. Functional outcomes and complications following radiation therapy for prostate cancer: a critical analysis of the literature. *Eur Urol*. 2012;61(1):112-127.

8. Spratt DE, Pei X, Yamada J, Kollmeier MA, Cox B, Zelefsky MJ. Long-term survival and toxicity in patients treated with high-dose intensity modulated radiation therapy for localized prostate cancer. *Int J Radiat Oncol Biol Phys*. 2013;85(3):686-692.
9. Lips IM, Kotte AN, van Gils CH, van Leerdam ME, van der Heide UA, van Vulpen M. Influence of antifatulent dietary advice on intrafraction motion for prostate cancer radiotherapy. *Int J Radiat Oncol Biol Phys*. 2011;81(4):e401-e406.
10. Nichol AM, Warde PR, Lockwood GA, et al. A cinematic magnetic resonance imaging study of milk of magnesia laxative and an antifatulent diet to reduce intrafraction prostate motion. *Int J Radiat Oncol Biol Phys*. 2010;77(4):1072-1078.
11. Keall PJ, Aun Ng J, O'Brien R, et al. The first clinical treatment with kilovoltage intrafraction monitoring (KIM): a real-time image guidance method. *Med Phys*. 2015;42(1):354-358.
12. Curtis W, Khan M, Magnelli A, Stephans K, Tendulkar R, Xia P. Relationship of imaging frequency and planning margin to account for intrafraction prostate motion: analysis based on real-time monitoring data. *Int J Radiat Oncol Biol Phys*. 2013;85(3):700-706.
13. Das S, Liu T, Jani AB, et al. Comparison of image-guided radiotherapy technologies for prostate cancer. *Am J Clin Oncol*. 2014;37(6):616-623.
14. Wu QJ, Li T, Yuan L, Yin FF, Lee WR. Single institution's dosimetry and IGRT analysis of prostate SBRT. *Radiat Oncol*. 2013;8:215.
15. Liu W, Luxton G, Xing L. A failure detection strategy for intrafraction prostate motion monitoring with on-board imagers for fixed-gantry IMRT. *Int J Radiat Oncol Biol Phys*. 2010;78(3):904-911.
16. Langen KM, Willoughby TR, Meeks SL, et al. Observations on real-time prostate gland motion using electromagnetic tracking. *Int J Radiat Oncol*. 2008;71(4):1084-1090.
17. Liu W, Wiersma RD, Mao W, Luxton G, Xing L. Real-time 3D internal marker tracking during arc radiotherapy by the use of combined MV-kV imaging. *Phys Med Biol*. 2008;53(24):7197-7213.
18. Kupelian P, Willoughby T, Mahadevan A, et al. Multi-institutional clinical experience with the Calypso System in localization and continuous, real-time monitoring of the prostate gland during external radiotherapy. *Int J Radiat Oncol Biol Phys*. 2007;67(4):1088-1098.
19. Lin Y, Liu T, Yang W, Yang X, Khan MK. The non-Gaussian nature of prostate motion based on real-time intrafraction tracking. *Int J Radiat Oncol Biol Phys*. 2013;87(2):363-369.
20. Xie YQ, Xing L, Gu J, Liu W. Tissue feature-based intrafractional motion tracking for stereoscopic X-ray image guided radiotherapy. *Phys Med Biol*. 2013;58(11):3615-3630.
21. Hunt MA, Sonnick M, Pham H, et al. Simultaneous MV-kV imaging for intrafractional motion management during volumetric-modulated arc therapy delivery. *J Appl Clin Med Phys*. 2016;17(2):5836.
22. Ma Y, Lee L, Keshet O, Keall P, Xing L. Four-dimensional inverse treatment planning with inclusion of implanted fiducials in IMRT segmented fields. *Med Phys*. 2009;36(6):2215-2221.
23. Zhao B, Dai J. Determining leaf trajectories for dynamic multileaf collimators with consideration of marker visibility: an algorithm study. *J Radiat Res*. 2014;55(5):976-987.
24. Lin WY, Lin SF, Yang SC, Liou SC, Nath R, Liu W. Real-time automatic fiducial marker tracking in low contrast cine-MV images. *Med Phys*. 2013;40(1):011715.
25. Zhang P, Mah D, Happersett L, Cox B, Hunt M, Mageras G. Determination of action thresholds for electromagnetic tracking system-guided hypofractionated prostate radiotherapy using volumetric modulated arc therapy. *Med Phys*. 2011;38(7):4001-4008.